Electronic Supplementary Material (ESI) for Nanoscale
This journal is © The Royal Society of Chemistry 2013

Electronic Supplementary Information

Modifying the Size and Uniformity of Upconversion Yb/Er: $NaGdF_4$ Nanocrystals through Alkaline-Earth Doping

Lei Lei, Daqin Chen*, Ping Huang, Ju Xu, Rui Zhang, Yuansheng Wang*

State Key Laboratory of Structural Chemistry,

Fujian Institute of Research on the Structure of Matter, Chinese Academy of Sciences, Fuzhou, Fujian, 350002 (P. R. China)

Corresponding Authors

dqchen@fjirsm.ac.cn (D. Q. Chen); yswang@fjirsm.ac.cn (Y. S. Wang)

Table S1-S2

Table S1 Lattice parameters, cell volume and mean size of xCa/20Yb/2Er: $NaGdF_4$ NCs

xCa/20Yb/2Er: $NaGdF_4$	Lattice parameters (Å)		Cell volume ($Å^3$)	Mean size (nm)
	a	*c*		
x=0	6.0131	3.6059	112.91	8
x=10	6.0093	3.6079	112.83	8
x=20	6.0061	3.6095	112.76	10
x=25	6.0125	3.6072	112.93	12
x=30	6.0102	3.6086	112.87	18
x=40	6.0109	3.6076	112.88	22

Table S2 UC efficiencies of xCa/20Yb/2Er: $NaGdF_4$ core NCs and xCa/20Yb/2Er: $NaGdF_4$@$NaYF_4$ core-shell NCs

Sample	Mean size (nm)	Power density (W/cm^2)	UC efficiency (%)
Yb/Er: $NaGdF_4$	8	2.5	0.015
Yb/Er: $NaGdF_4$@$NaYF_4$	11	2.5	0.051
Ca/Yb/Er: $NaGdF_4$	18	2.5	0.072
Ca/Yb/Er: $NaGdF_4$@$NaYF_4$	24	2.5	2.300

Figure S1-S24

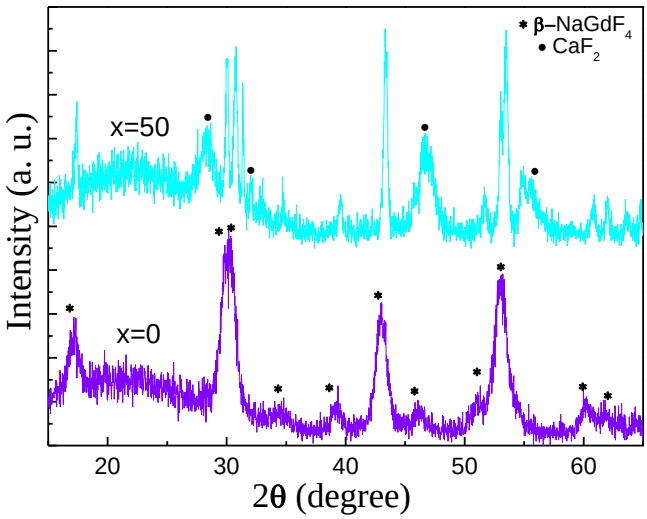

Figure S1 XRD patterns of xCa/20Yb/2Er: $NaGdF_4$ NCs: (x=0, 50 mol%).

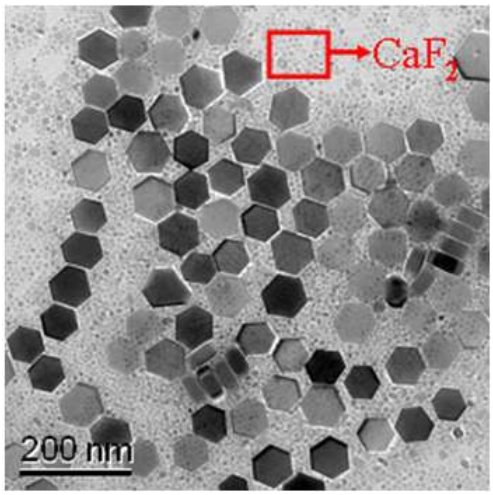

Figure S2 TEM micrograph of 50Ca/20Yb/2Er: $NaGdF_4$ NCs.

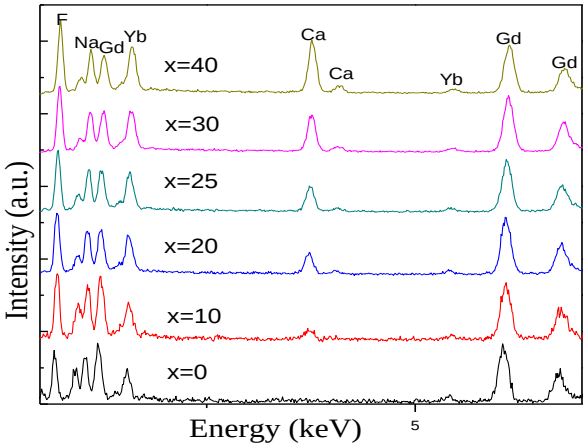

Figure S3 EDS spectra of xCa/20Yb/2Er: $NaGdF_4$ (x=0, 10, 20, 25, 30, 40 mol%) NCs, all the signals are normalized to Gd one, and Cu signals come from copper grid.

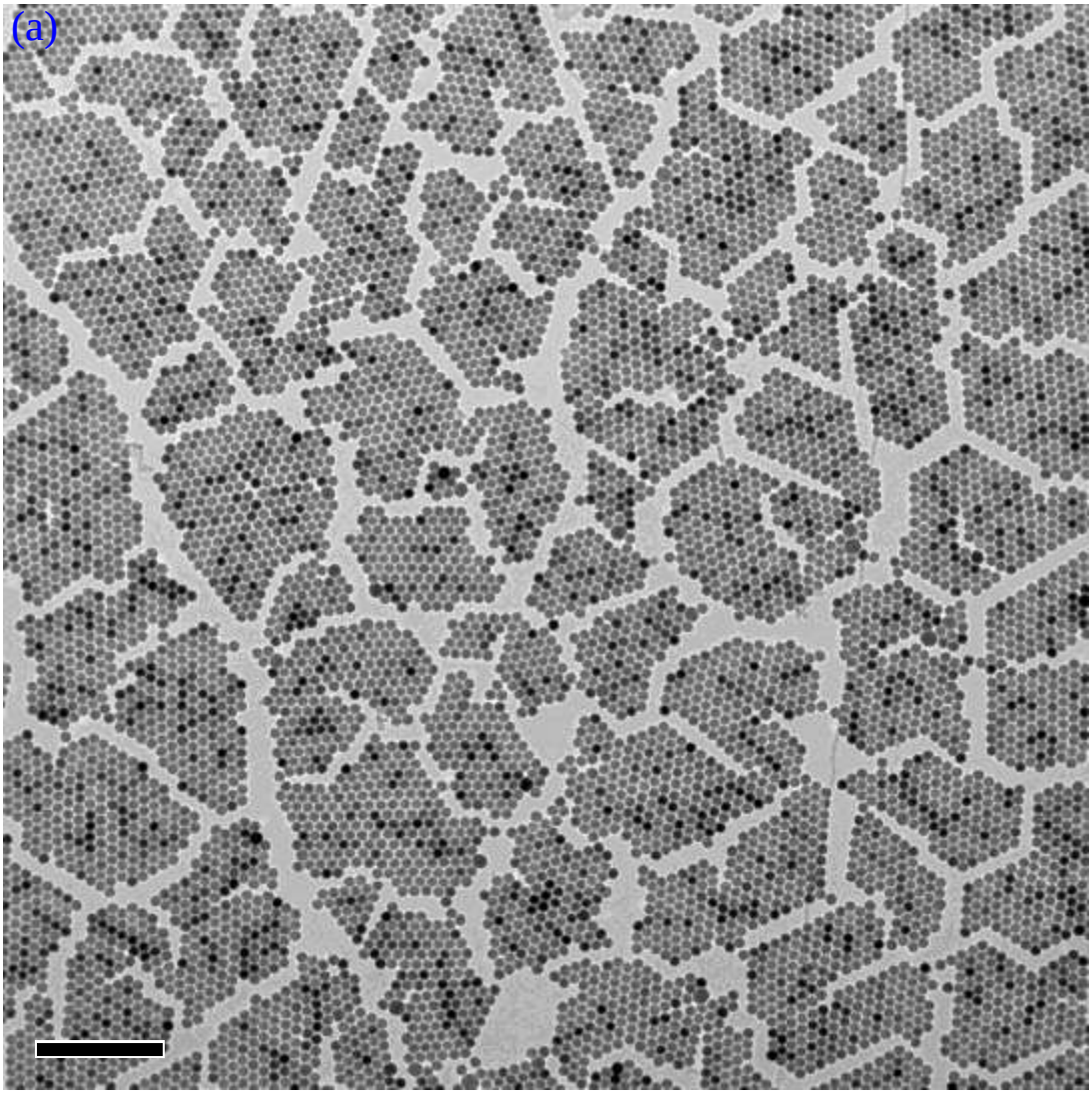
(a)

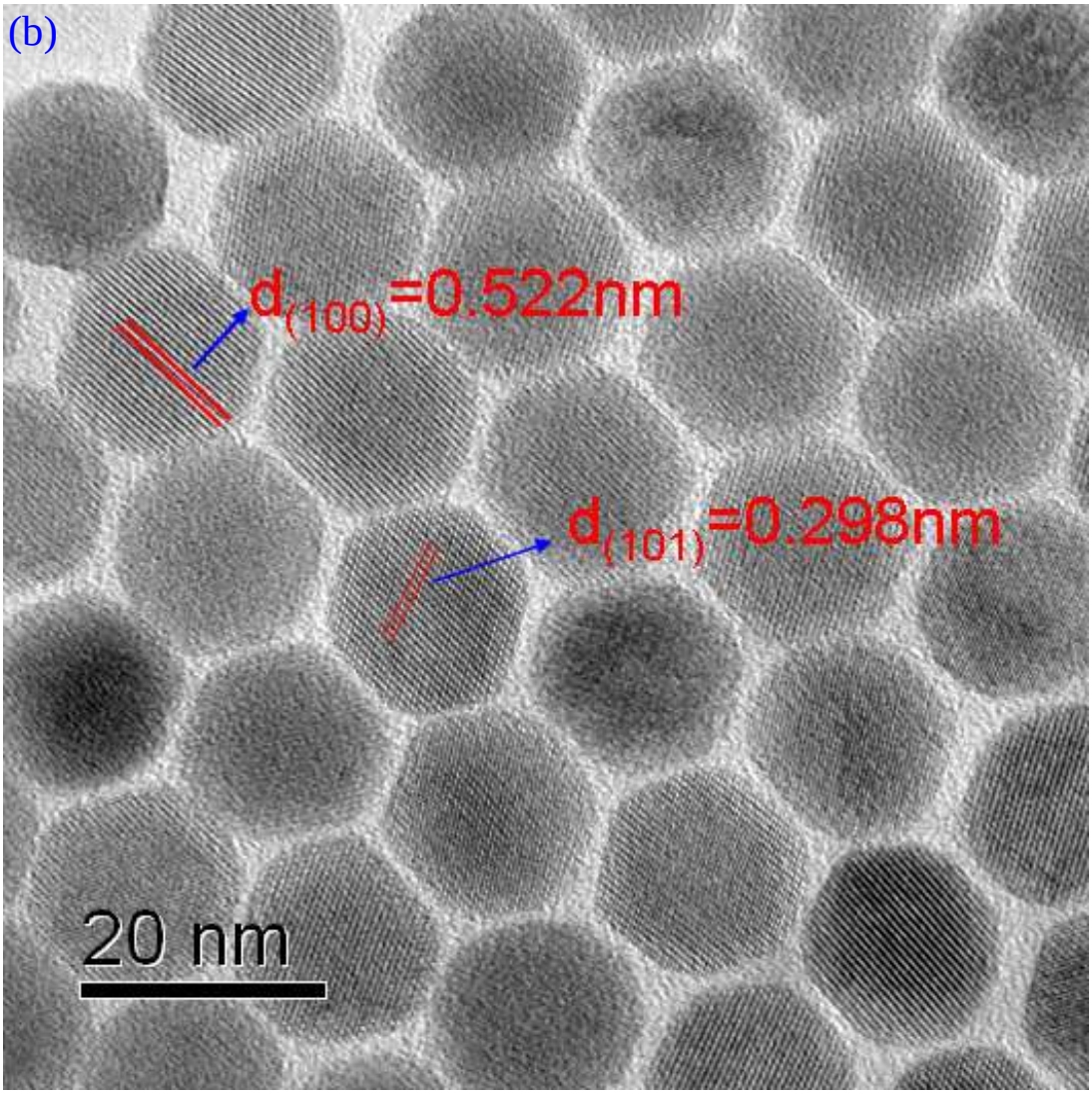

Figure S4 TEM images of 30Ca/20Yb/2Er: $NaGdF_4$ NCs with (a) low-, and (b) high-magnifications.

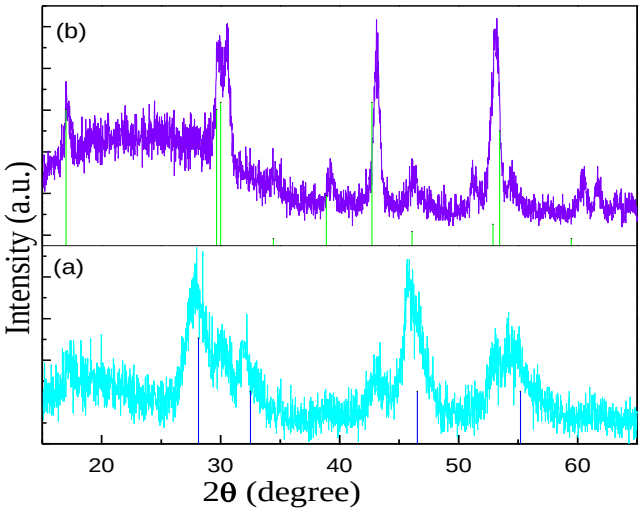

Figure S5 XRD patterns of xCa/20Yb/2Er: $NaGdF_4$ NCs synthesized under 280 ºC for 30 min: (a) x=0, (b) 30 mol%; Bars in (a) and (b) represent standard cubic $NaGdF_4$ (JCPDS 27-0697) and hexagonal $NaGdF_4$ (JCPDS27-0699) crystal data, respectively.

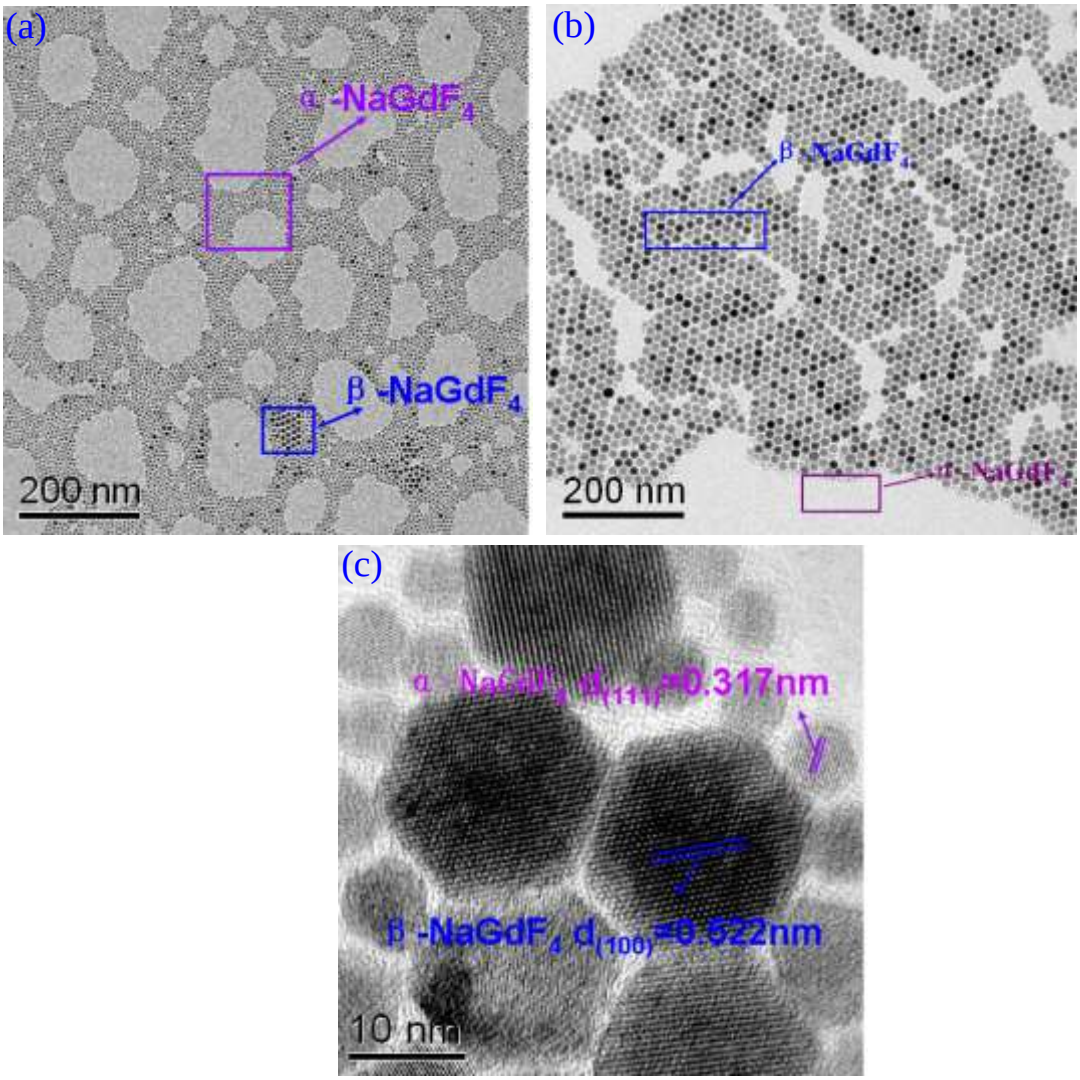

Figure S6 TEM micrographs of (a) Yb/Er: $NaGdF_4$ and Ca^{2+}-doped Yb/Er: $NaGdF_4$ NCs synthesized at 280 ºC for 30 min; (c) HRTEM image of sample (b).

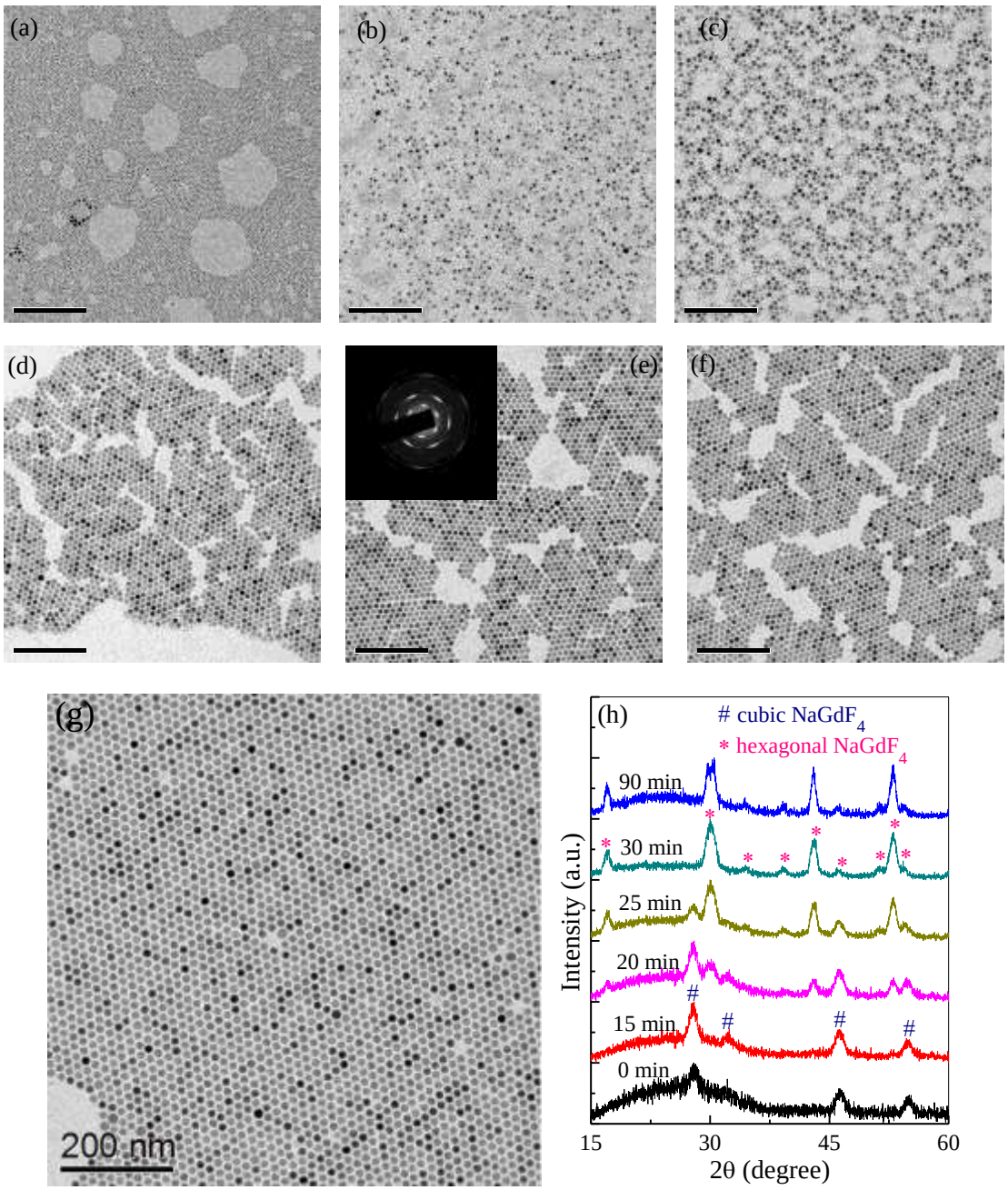

Figure S7 TEM micrographs of 30 mol% Ca^{2+}-doped Yb/Er: $NaGdF_4$ NCs prepared at 280 ºC for different durations: (a) 15 min, (b) 20 min, (c) 25 min, (d) 30 min, (e) 40 min, (f) 60 min, and (g) 90 min; inset of (e) is the corresponding SAED pattern; (h) XRD patterns of 30Ca/20Yb/2Er: $NaGdF_4$ NCs prepared at 280 ºC for different durations.

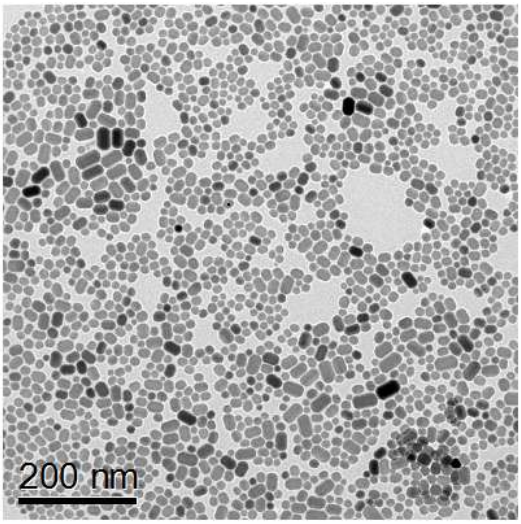

Figure S8 TEM micrograph of Yb/Er: $NaGdF_4$ NCs synthesized at 300 ºC for 90 min.

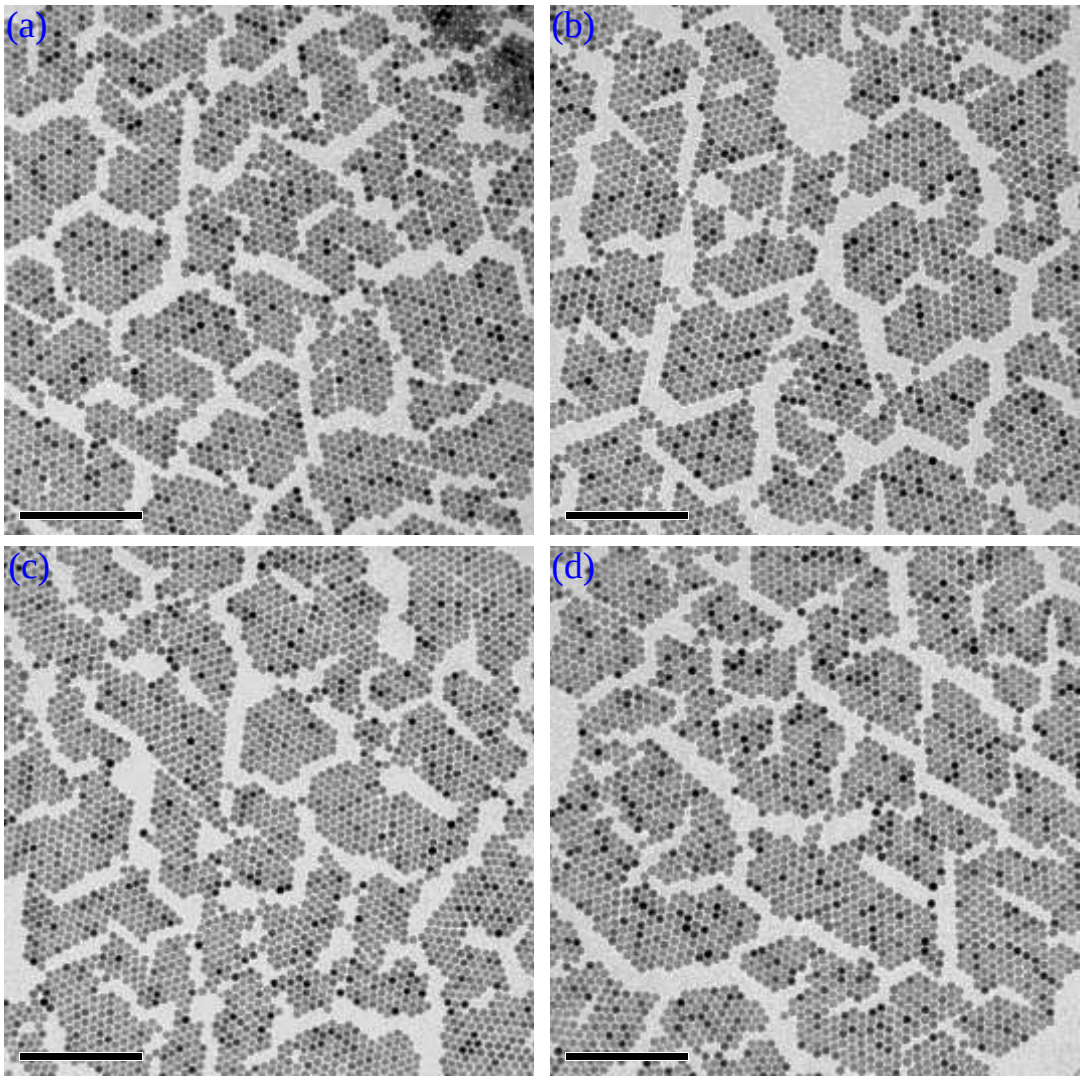

Figure S9 TEM imicrographs of 30 mol% Ca^{2+}-doped Yb/Er: $NaGdF_4$ NCs synthesized at 300 ºC for different durations: (a) 90 min, (b) 3h, (c) 6h, and (d) 12h.

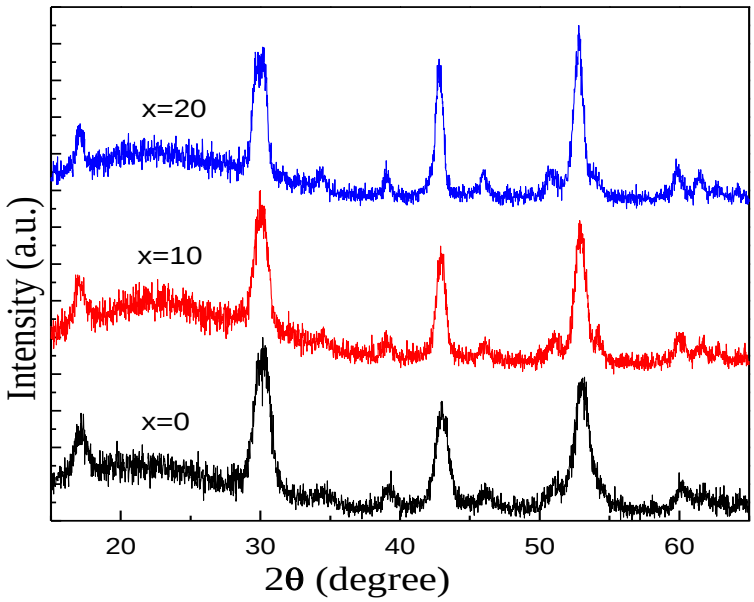

Figure S10 XRD patterns of xSr/20Yb/2Er: $NaGdF_4$ NCs: (x=0, 10, and 20 mol%).

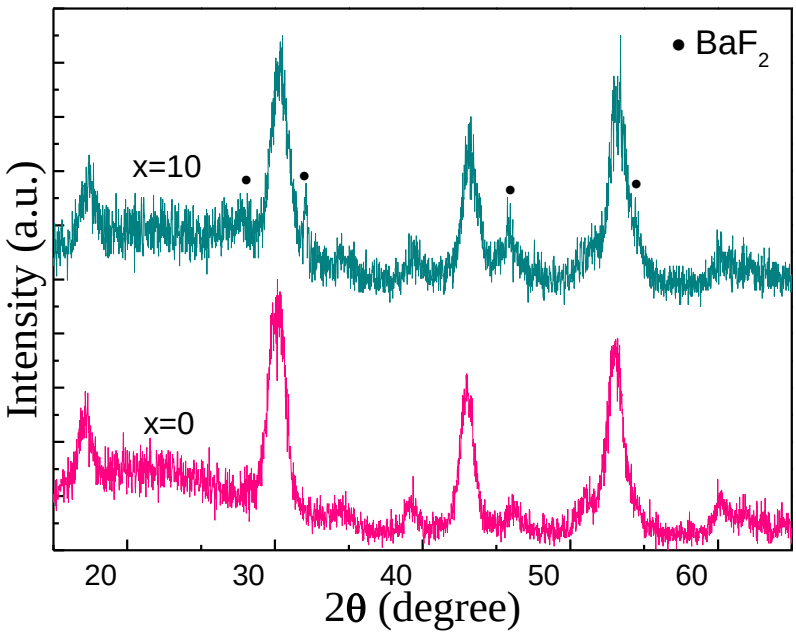

Figure S11 XRD patterns of xBa/20Yb/2Er: $NaGdF_4$ NCs: (x=0, 10 mol%).

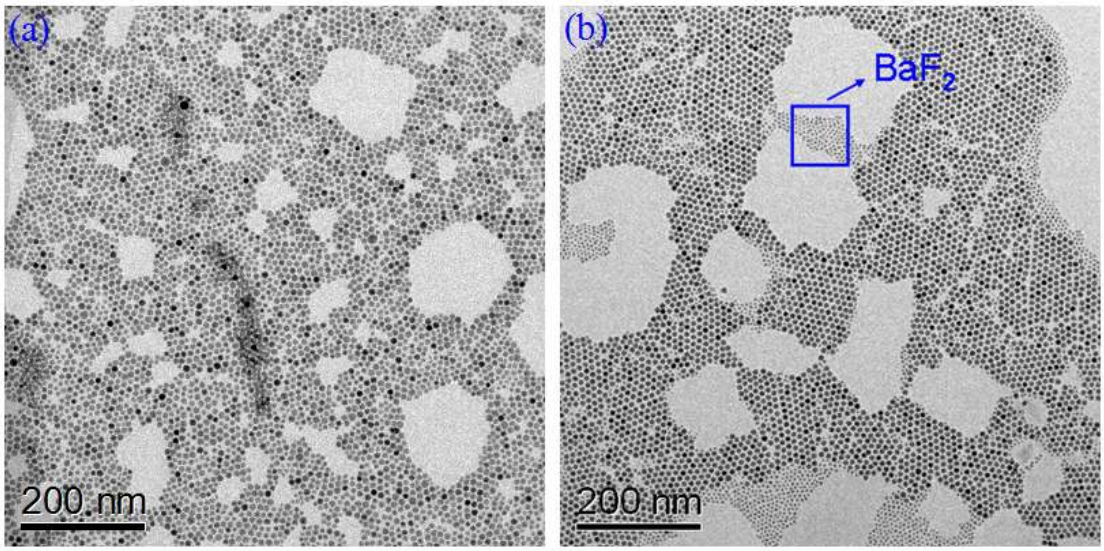

Figure S12 TEM micrographs of xBa/20Yb/2Er: $NaGdF_4$ NCs: (a) x=0, (b) x=10.

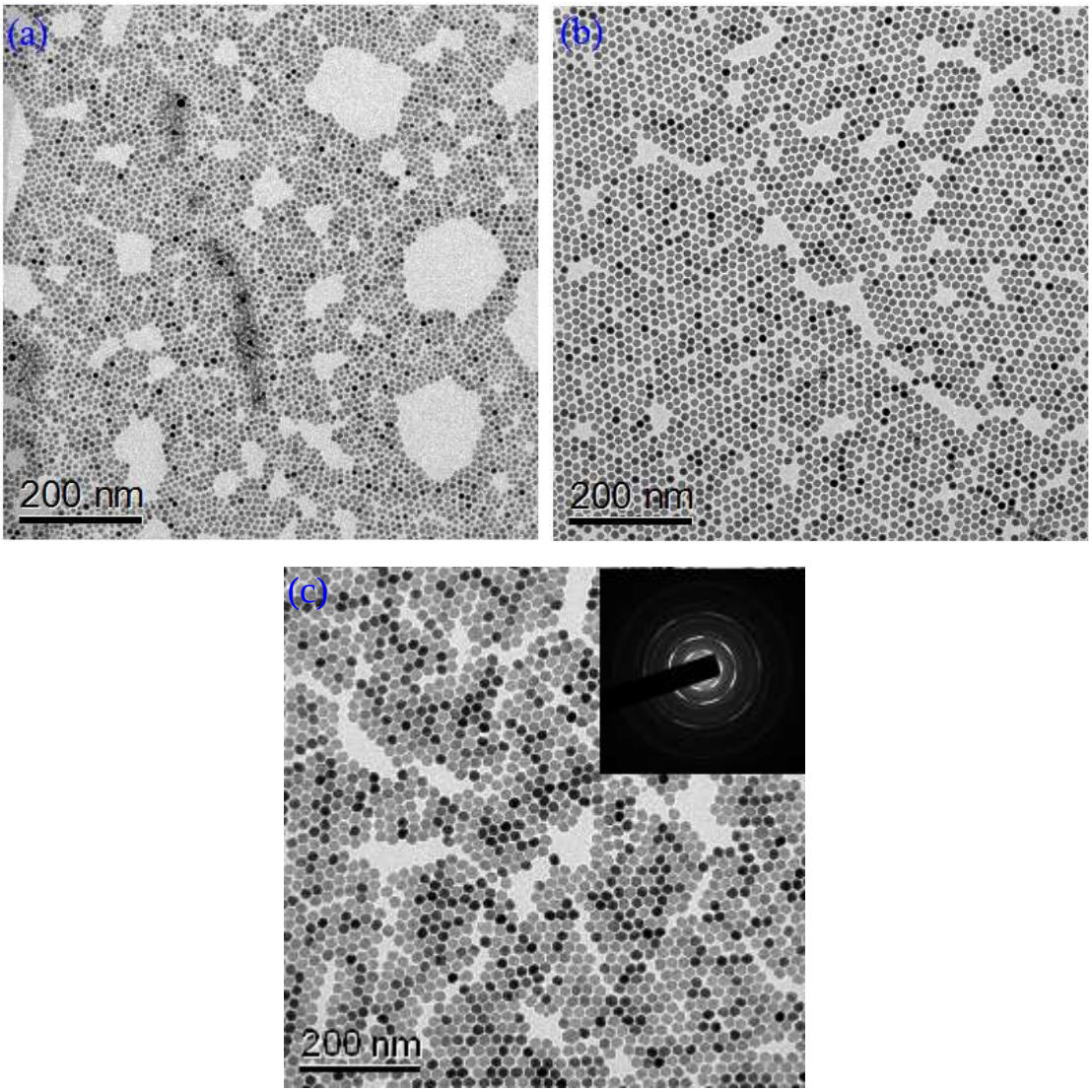

Figure S13 TEM micrographs of xSr/20Yb/2Er: $NaGdF_4$ NCs: (a) x=0, (b) x=10 and (c) x=20; inset of (c) is the corresponding SAED pattern.

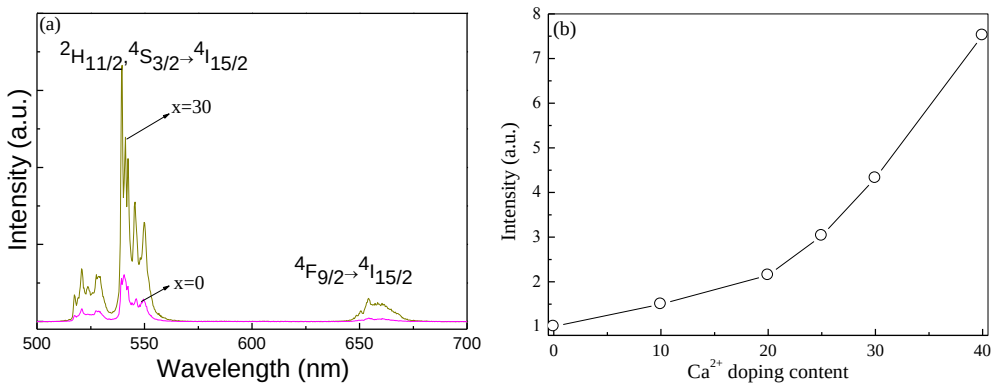

Figure S14 (a) UC emission spectra of xCa/20Yb/2Er: $NaGdF_4$ NCs (x=0, 30 mol%) under 976 nm excitation; (b) UC emission intensity versus Ca^{2+} doping content.

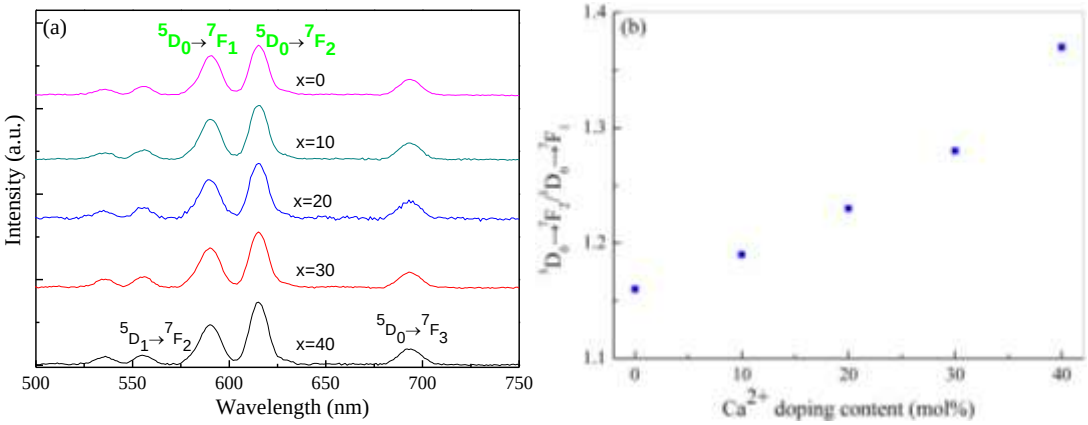

Figure S15 (a) Photoluminescence spectra of xCa/5Eu: $NaGdF_4$ (x=0, 10, 20, 30, 40 mol%) NCs under 395 nm excitation, (b) dependence of emission intensity ratio ($^5D_0$ →$^7F_2$ /$^5D_0$→$^7F_1$) on Ca^{2+} doping content.

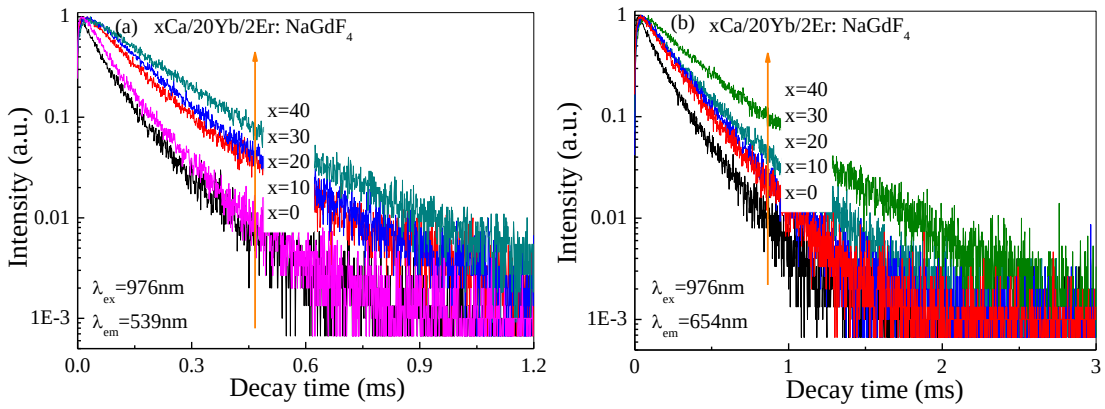

Figure S16 UC luminescent decay curves of xCa/20Yb/2Er: $NaGdF_4$ (x=0, 10, 20, 30, 40 mol%) NCs: (a) the $^4S_{3/2}$→$^4I_{15/2}$ and (b) $^4F_{9/2}$→$^4I_{15/2}$ transitions of Er^{3+}.

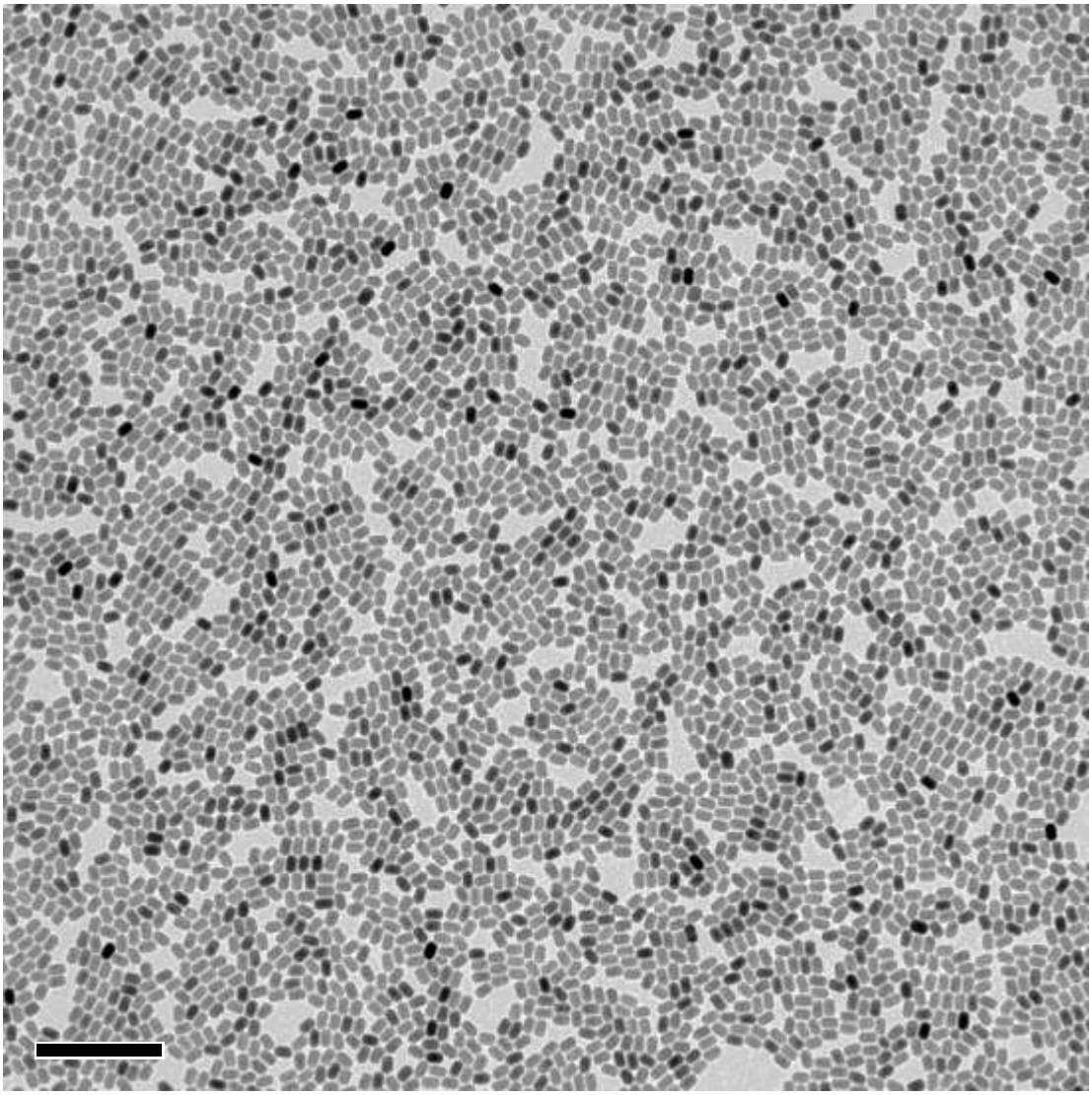

Figure S17 TEM micrograph of 30Ca/20Yb/2Er: $NaGdF_4$@$NaYF_4$ core-shell particles with low-magnification.

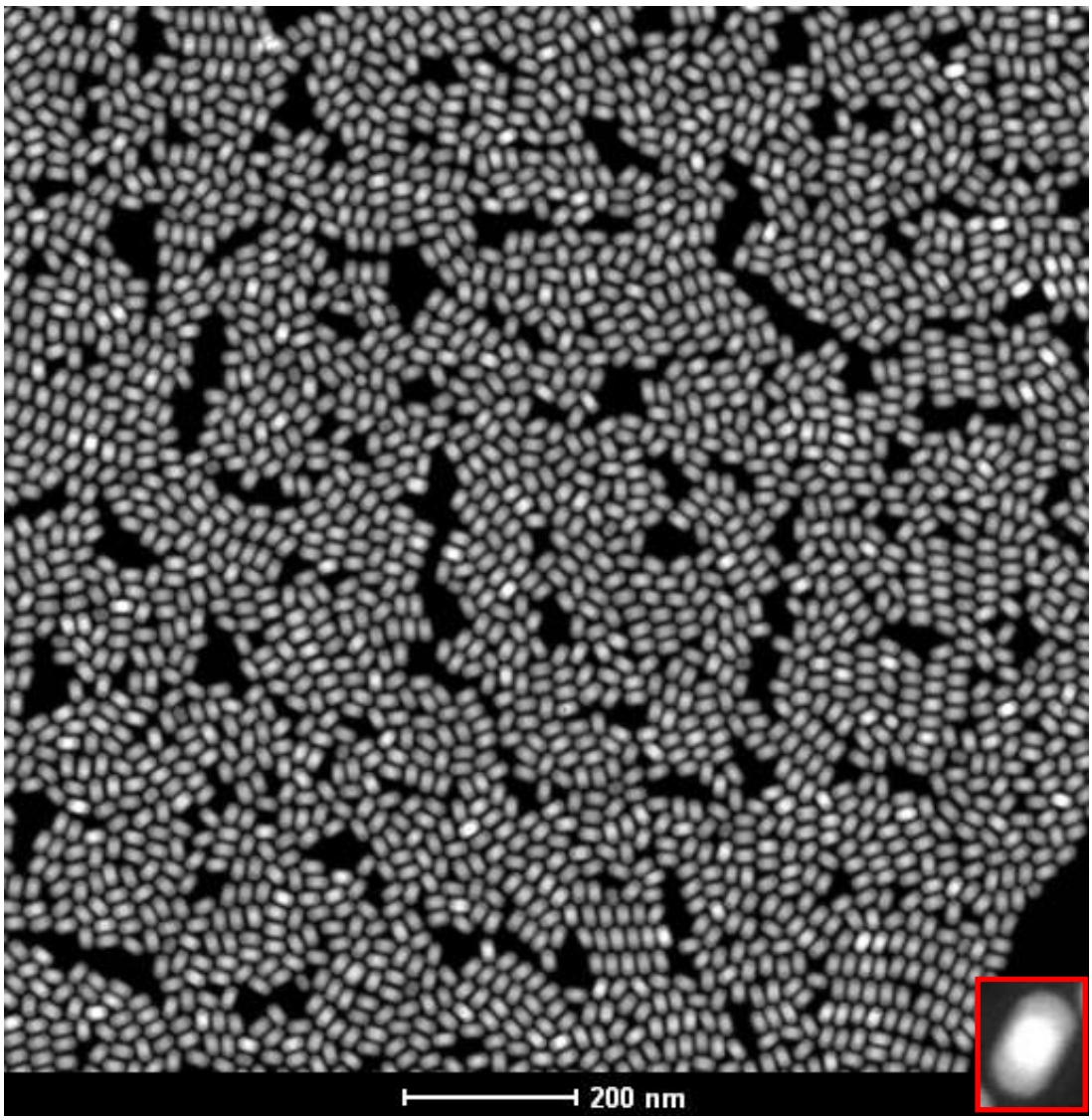

Figure S18 STEM-HAADF image of 30Ca/20Yb/2Er: $NaGdF_4$@$NaYF_4$ core-shell particles with low-magnification.

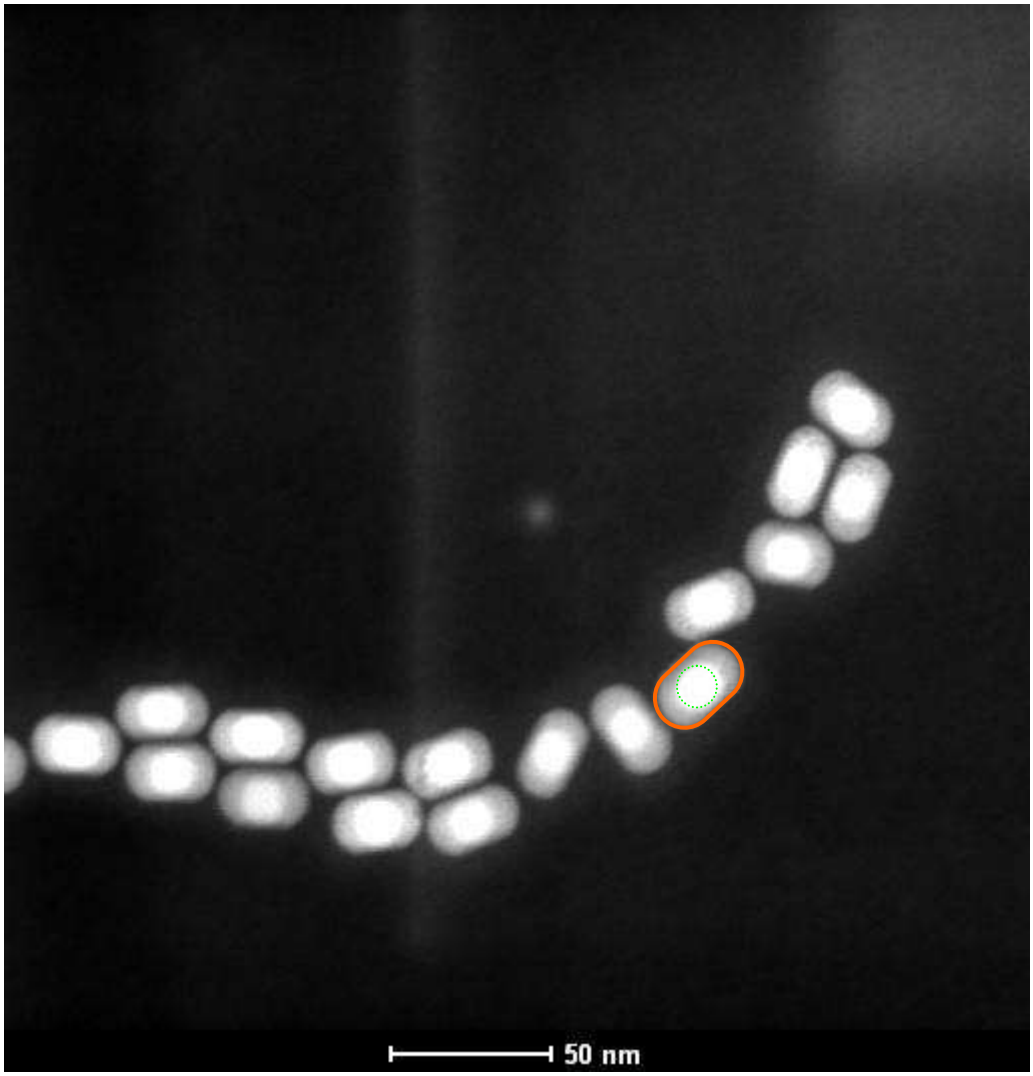

Figure S19 High-contrast STEM-HAADF image of Ca/Yb/Er: $NaGdF_4$@$NaYF_4$ core-shell particles.

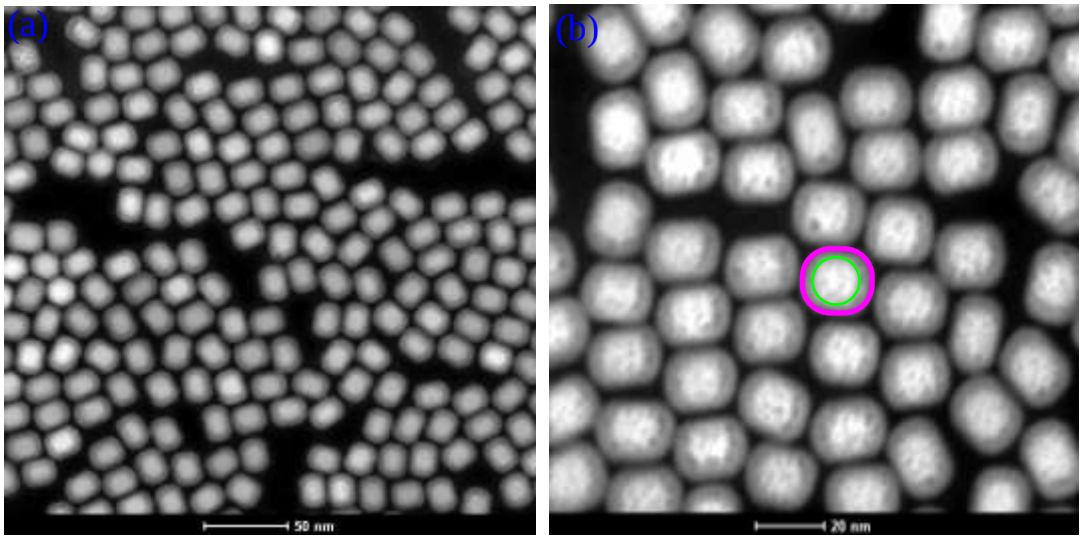

Figure S20 Low- and high-magnification STEM-HAADF images of Ca/Yb/Er: $NaGdF_4$@$NaYF_4$ core-shell particles fabricated by using high ratio of shell precursors to core NCs in solution.

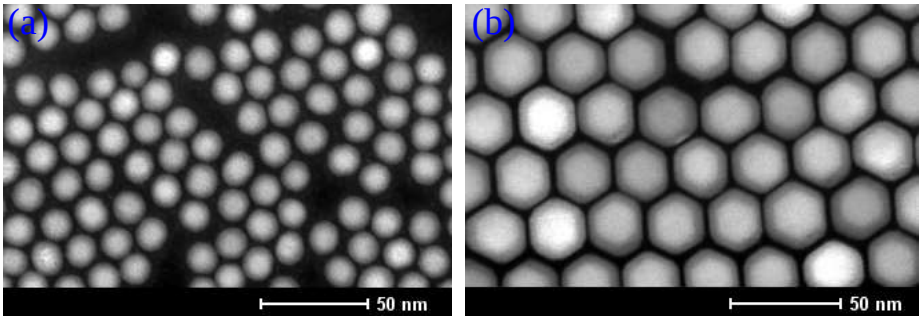

Figure S21 STEM-HAADF images of (a) 10Ca/20Yb/2Er: $NaGdF_4$@$NaYF_4$ and (b) 40Ca/20Yb/2Er: $NaGdF_4$@$NaYF_4$ Core-shell NCs.

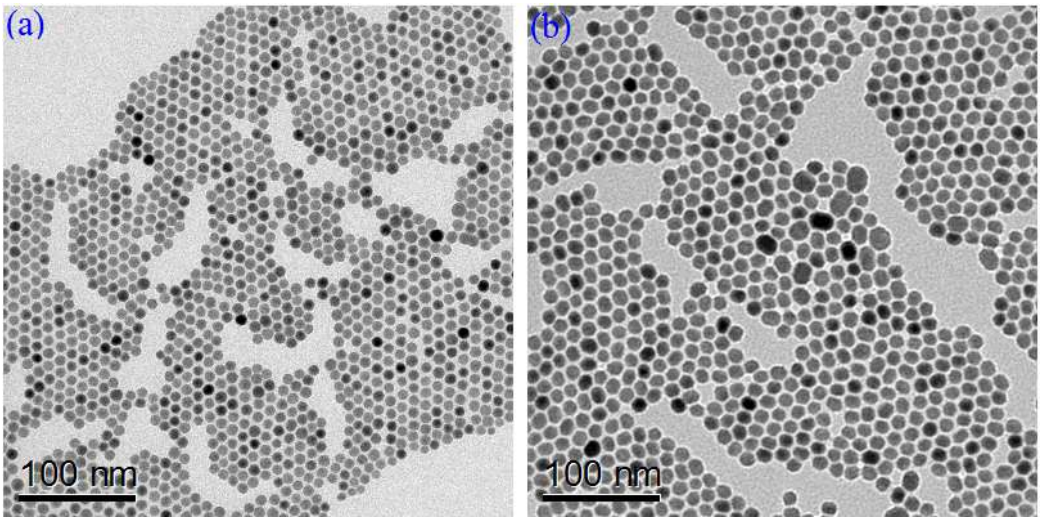

Figure S22 TEM micrographs of (a) Yb/Er: $NaGdF_4$ cores and (b) Yb/Er: $NaGdF_4$@$NaYF_4$ core-shell particles.

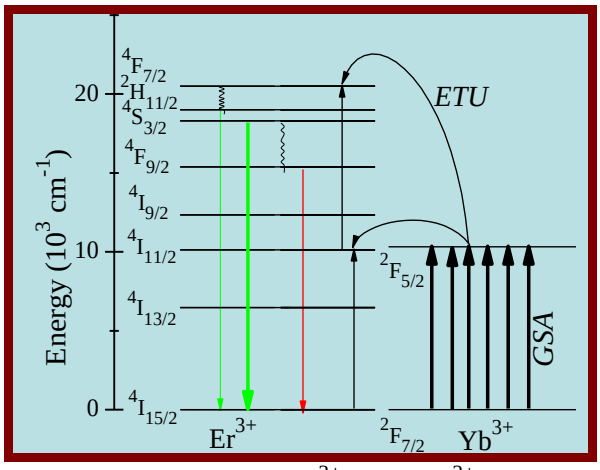

Figure S23 Energy level diagrams of Er^{3+} and Yb^{3+} ions, showing possible energy transfer mechanisms for red and green UC emissions of Er^{3+} activators in the hosts; GSA and ETU represent ground state absorption and energy transfer upconversion, respectively.

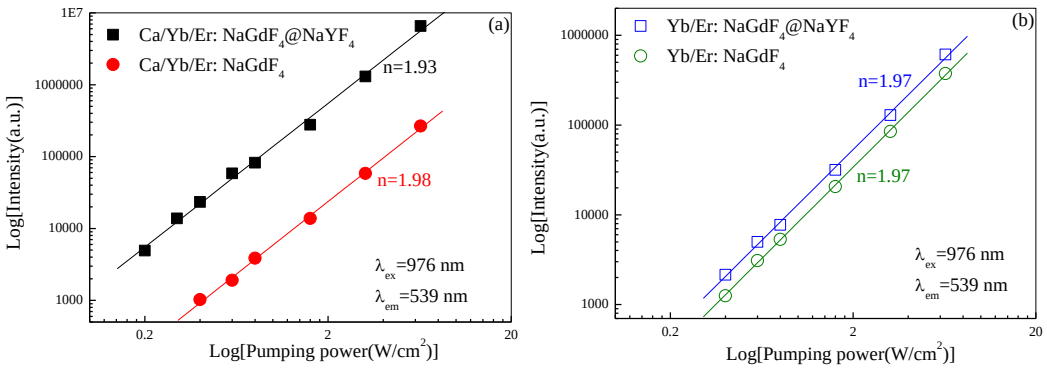

Figure S24 Log-log plots of UC emission intensity versus pumping power of the products: (a) Ca/Yb/Er: $NaGdF_4$ core and Ca/Yb/Er: $NaGdF_4$@$NaYF_4$ core-shell particles; (b) Yb/Er: $NaGdF_4$ core and Yb/Er: $NaGdF_4$@$NaYF_4$ core-shell particles.